Check for updates

Received: 16 August 2021 | Revised: 26 October 2021 | Accepted: 30 November 2021

DOI: 10.1111/jnc.15553

Journal of Neurochemistry JNC The Official Journal of the International Society for Neurochemistry WILEY

ORIGINAL ARTICLE

Hydromethylthionine enhancement of central cholinergic signalling is blocked by rivastigmine and memantine

Constantin Kondak[1,2] | Gernot Riedel[1] | Charles R. Harrington[1,3] | Claude M. Wischik[1,3] | Jochen Klein[2]

[1]Institute of Medical Sciences, Translational Neuroscience, University of Aberdeen, Aberdeen, Scotland

[2]Institute of Pharmacology and Clinical Pharmacy, Goethe University Frankfurt, Frankfurt, Germany

[3]TauRx Therapeutics Ltd, Aberdeen, Scotland

Correspondence
Jochen Klein, Institute of Pharmacology and Clinical Pharmacy, Goethe University Frankfurt, Max-von-Laue-Str. 9, 60438 Frankfurt, Germany.
Email: klein@em.uni-frankfurt.de

Funding information
TauRx Therapeutics Ltd., Aberdeen, Grant/Award Number: R0154

Abstract

The prevention of tau protein aggregations is a therapeutic goal for the treatment of Alzheimer's disease (AD), and hydromethylthionine (HMT) (also known as leucomethylthioninium-mesylate [LMTM]), is a potent inhibitor of tau aggregation *in vitro* and *in vivo*. In two Phase 3 clinical trials in AD, HMT had greater pharmacological activity on clinical endpoints in patients not receiving approved symptomatic treatments for AD (acetylcholinesterase (AChE) inhibitors and/or memantine) despite different mechanisms of action. To investigate this drug interaction in an animal model, we used tau-transgenic L1 and wild-type NMRI mice treated with rivastigmine or memantine prior to adding HMT, and measured changes in hippocampal acetylcholine (ACh) by microdialysis. HMT given alone doubled hippocampal ACh levels in both mouse lines and increased stimulated ACh release induced by exploration of the open field or by infusion of scopolamine. Rivastigmine increased ACh release in both mouse lines, whereas memantine was more active in tau-transgenic L1 mice. Importantly, our study revealed a negative interaction between HMT and symptomatic AD drugs: the HMT effect was completely eliminated in mice that had been pre-treated with either rivastigmine or memantine. Rivastigmine was found to inhibit AChE, whereas HMT and memantine had no effects on AChE or on choline acetyltransferase (ChAT). The interactions observed in this study demonstrate that HMT enhances cholinergic activity in mouse brain by a mechanism of action unrelated to AChE inhibition. Our findings establish that the drug interaction that was first observed clinically has a neuropharmacological basis and is not restricted to animals with tau aggregation pathology. Given the importance of the cholinergic system for memory function, the potential for commonly used AD drugs to interfere with the treatment effects of disease-modifying drugs needs to be taken into account in the design of clinical trials.

KEYWORDS
acetylcholine, Alzheimer's disease, hippocampus, hydromethylthionine, memantine, microdialysis, rivastigmine

Abbreviations: aCDF, artificial cerebrospinal fluid; ACh, acetylcholine; AChE, acetylcholinesterase; AD, Alzheimer´s disease; ChAT, choline acetyltransferase; GABA, gamma-aminobutyric acid; HMT, hydromethylthionine; LMTM, leucomethylthioninium dihydromesylate; MTC, methylthioninium chloride (methylene blue); PHF, paired helical filaments.

This is an open access article under the terms of the Creative Commons Attribution License, which permits use, distribution and reproduction in any medium, provided the original work is properly cited.
© 2021 The Authors. *Journal of Neurochemistry* published by John Wiley & Sons Ltd on behalf of International Society for Neurochemistry

1 | INTRODUCTION

Central cholinergic transmission via its predominantly excitatory neurotransmitter acetylcholine (ACh) is pivotal for memory formation and learning processes (Hasselmo, 2006; Sarter & Lustig, 2019; Thiele, 2013). Cholinergic innervation arising from basal forebrain, namely the medial septum, the diagonal band of Broca and the nucleus basalis of Meynert, projects directly into the neocortex and the limbic system, which includes the hippocampus and the entorhinal cortex (Mesulam & van Hoesen, 1976; Sakanaka et al., 1980). The latter brain areas are part of the Papez neuron circuit, which drives functional changes in hippocampal pyramidal cells and represents the structural basis for consolidation of memory (Vertes et al., 2001). Notably, signalling in the limbic system is not exclusively cholinergic, but is modulated by GABAergic interneurons and glutamatergic transmission (Bonanno et al., 1991; Giovannini et al., 1994).

The indispensable role of cholinergic signalling in memory processing is evident in Alzheimer's disease (AD), which is characterised by memory loss and cognitive decline and is accompanied by a marked and progressive degeneration of cholinergic neurons (Arendt et al., 1999; Schliebs & Arendt, 2006; Zimmermann, 2020). The cholinergic innervation originating in the basal forebrain and projecting to cortico-limbic areas declines severely in AD (Mesulam, 2013; Vana et al., 2011; Whitehouse et al., 1981). Furthermore, autopsied brains of AD patients show a reduction in presynaptic markers, such as choline acetyltransferase (ChAT) activity, in the limbic system and cerebral cortex (Hampel et al., 2018; Mesulam, 2013; Pepeu & Grazia Giovannini, 2017). These findings implicate a loss of cholinergic terminals in those areas.

The rationale for treatments aiming to counteract the cholinergic deficit seen in AD by acetylcholinesterase (AChE) inhibition appears reasonable. The approved drugs, namely donepezil, galantamine and rivastigmine, are capable of reducing symptoms initially, but they have limited long-term therapeutic value (Kaduszkiewicz et al., 2005). Memantine, an NMDA receptor antagonist developed to reduce neurodegeneration, was approved by the FDA for AD nearly two decades ago (Cummings et al., 2014). However, memantine also fails to provide adequate AD therapy. In fact, several meta-analyses have expressed considerable doubt about the clinical benefit of memantine treatment (Blanco-Silvente et al., 2018; McShane & Schneider, 2005; Schneider et al., 2011).

Further therapeutic approaches have targeted different species of aggregated protein structures which accompany neurodegeneration in AD (Ower et al., 2018). Increased formation and insufficient degradation of amyloid-β (Aβ) leads to extracellular plaques, but pharmacological treatments aiming to dissolve or prevent these aggregates have failed to improve cognitive abilities in numerous clinical studies (Anderson et al., 2017). The FDA recently approved an anti-amyloid monoclonal antibody on the basis of reduction in amyloid load on the brain alone, but without clear evidence of clinical benefit. Intracellular tau aggregates were described early in AD (Ginsberg et al., 2006; Mena et al., 1995; Wischik et al., 1988) and were used by Braak to stage the progression of neurodegeneration (Braak & Braak, 1991). Starting in entorhinal cortex, tau aggregation affects the hippocampus (including cholinergic axons and terminals) and other neocortical regions, leading to the accumulation of insoluble paired helical filaments (PHFs) which are composed of tau protein (Wischik et al., 1988, 1995). As tau has a crucial role in axonal transport, its functional absence because of aggregation has severe implications for neuronal health and arguably is a sufficient driver of dementia pathology (Spillantini & Goedert, 2013; Wischik et al., 1995). Moreover, post-mortem studies suggest that tau aggregates are responsible for neurodegeneration in the nucleus basalis of Meynert and subsequently for the loss of cholinergic input into the cortical system (Braak & Del Tredici, 2013; Geula et al., 2008; Mesulam, 2013). In our hands, amyloid overexpression did not affect central cholinergic systems in mice (Hartmann et al., 2010), whereas tau-transgenic mice had reduced acetylcholine levels (Stein et al., 2019). Accordingly, tau-directed therapies have recently attracted increasing attention in the AD field.

Methylthioninium chloride (MTC, commonly known as methylene blue) was the first selective tau aggregation inhibitor *in vitro* (Wischik et al., 1996). MTC treatment was found to slow cognitive decline at a dose of 138 mg/day as monotherapy in a phase 2 trial in AD (Wischik et al., 2015). A reduced form of this compound, hydromethylthionine (HMT; the new International Non-Proprietary Name for leucomethylthioninium, LMT), as the dihydromesylate salt (LMTM), was tested in two phase 3 trials in mild to moderate AD treatment in which doses in the range 150–250 mg/day were compared with a low dose of 8 mg/day intended as an inactive control. There were no differences between high and low doses in either of the two trials (Gauthier et al., 2016; Wilcock et al., 2018). The lack of dose-dependent difference has since been explained by the fact that, in contrast to MTC, 8 mg/day is the minimum effective dose of HMT and there is a response plateau at higher levels of exposure (Schelter et al., 2019). Highly significant differences were seen in both trials between patients receiving HMT as monotherapy and those receiving HMT as an add-on to standard symptomatic treatments (Gauthier et al., 2016; Wilcock et al., 2018). In the present study, we have investigated how prototypic symptomatic drugs (rivastigmine and memantine) modify cholinergic signalling responses to HMT in murine hippocampus. We have used microdialysis measurements of ACh levels and measurements of AChE and choline acetyltransferase (ChAT) activities to compare responses to HMT and symptomatic drugs alone and in combination in wild-type and tau transgenic mice expressing the core tau unit of the PHF (Melis, Zabke, et al., 2015).

2 | METHODS

2.1 | Animal model

The transgenic line 1 (L1) mouse expresses a truncated core PHF-tau fragment that consists of tau296–390 from the longest human CNS tau isoform htau40 on an NMRI background. Under control

14714159, 2022, 2, Downloaded from https://onlinelibrary.wiley.com/doi/10.1111/jnc.15553 by Test, Wiley Online Library on [30/07/2024]. See the Terms and Conditions (https://onlinelibrary.wiley.com/terms-and-conditions) on Wiley Online Library for rules of use; OA articles are governed by the applicable Creative Commons License

of the Thy1 regulatory element, expression of the transgene leads to the accumulation of oligomeric tau in the absence of intracellular neurofibrillary tangles (Melis, Zabke, et al., 2015). In mice up to 6 months of age the tau protein aggregates were found in hippocampus and entorhinal cortex. By 12–18 months of age, tau aggregates spread to further cortical structures, such as visual and retrosplenial cortex. The neuroanatomical distribution and the progressive spreading of these aggregates occur in a pattern similar to the Braak staging of tau pathology in AD (Braak & Braak, 1991). Cognitive deficits were moderate in younger mice (up to 3 months) and increased with higher age (6 months); significant impairments in sensorimotor function were not observed (Melis, Zabke, et al., 2015). In the present study, we used mice at 6–8 months of age because tau pathology was fully developed at this age and learning deficits were significant (Melis, Magbagbeolu, et al., 2015; Melis, Zabke, et al., 2015).

2.2 | Animals and drug treatment

A total of 120 female mice (60 NMRI (RRID:IMSR_TAC:nmri) and 60 L1, 6–8 months old, delivered by Charles River) were housed in groups of 5 or 6 in stock boxes prior to testing. Animals had access to food and water *ad libitum* and were kept under standard conditions (temperature 20–22°C, 50–65% relative humidity; 17–20 air changes per hour) and on a 12-h light/dark cycle (07:00 AM to 07:00 PM). After at least 1 week of habituation to the animal facility, mice were randomly assigned to study groups (10 per group) by using block randomisation (Latin square design). Based upon five or six animals per cage, mice were assigned to either five or six groups in the following order: ABCDE, BAECD, CDAEB, DEBAC, ECDBA or ABCDEF, BFDCAE, CDEFBA, DAFECB, ECABFD, and FEBADC. All animal procedures were carried out to minimise animal suffering in accordance with German and European law (EU directive 2010/63/EU). Exclusion criteria were death during anaesthesia, blocked microdialysis probes, probe leaking, or animals under severe pain. Three mice of different genetic background died because of respirational failure during surgery, another nine had to be excluded because of probe leakage. Three mice were tested on day one but were excluded on day two because of blocked probes. The study was registered with the local authorities (RP Darmstadt; FR1011).

HMT was synthesised in-house; its chemical characterisation has been reported (Baddeley et al., 2015). HMT (TauRx Therapeutics Ltd.) was stored at 8°C. Immediately before administration it was dissolved in nitrogen-sparged water to minimise oxidation. Rivastigmine (Tocris Bioscience; Cat. 129101-54-8) and memantine (Tocris Bioscience; Cat. 41100-52-1) were diluted in *aqua ad injectabilia* prior to filling minipumps.

Figure 1 shows the different groups and therapy regimes. Rivastigmine (0.5 mg/kg/d) and memantine (1 mg/kg/d) were delivered via an osmotic minipump (ALZET® pump model 1004; DURECT) which was implanted 4 weeks before dialysis. After filling, the pump was placed subcutaneously in the back region and the small incisional wound was sealed with wound closure clips (FST). This procedure was sufficient to deliver the drug constantly for at least 28 days. The doses were selected according to a previous study in our lab (Deiana et al., 2009) or converted from human doses using a dose conversion routine (Nair & Jacob, 2016).

Saline (0.2 ml/day) or HMT (5 mg/kg/day) were given daily by oral gavage for 2 weeks prior to the experiment. Drugs and chemicals of general use were supplied by Merck or Sigma at the highest purity available.

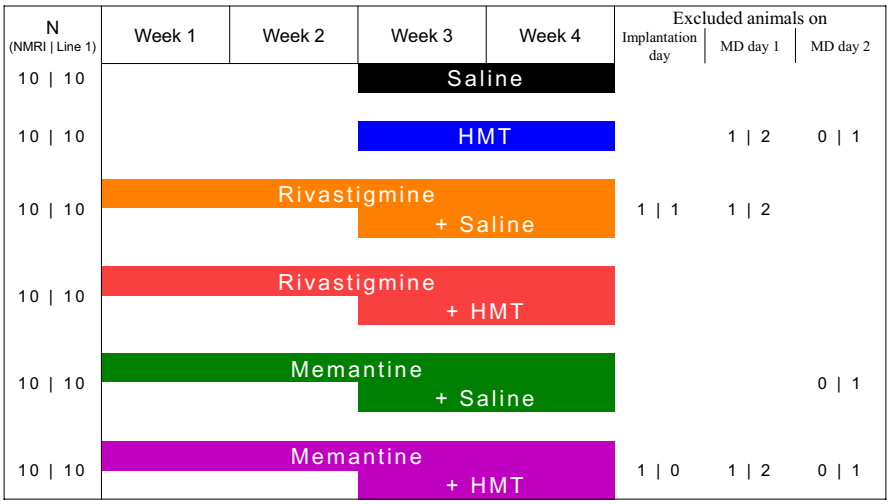

FIGURE 1 Administration regime for different drug treatments. Rivastigmine (0.5 mg/kg/d) and memantine (1 mg/kg/d) were administered using an osmotic mini-pump, which was implanted 28 days prior to the experiments. Saline (0.2 ml/kg/d) or HMT (5 mg/kg/d) were given daily by oral gavage in the last 2 weeks before the experiment, starting on day 15. Probe implantation was done on day 26, following two consecutive days of microdialysis experiments. For each group, a number of 10 animals was intended. The exact number of animals for each experiment is given in the respective figure description

14714159, 2022, 2, Downloaded from https://onlinelibrary.wiley.com/doi/10.1111/jnc.15553 by Test, Wiley Online Library on [30/07/2024]. See the Terms and Conditions (https://onlinelibrary.wiley.com/terms-and-conditions) on Wiley Online Library for rules of use; OA articles are governed by the applicable Creative Commons License

2.3 | Microdialysis

Prior to probe implantation mice were single housed in microdialysis cages in the experimental room. A habituation phase of at least 1 h was left before the surgery started. Self-built probes (Lietsche et al., 2014) were tested for leakage and recovery of ACh, which was found to be 12.2 ± 3.0% (N = 20). The microdialysis membrane (Filtral 12 AN69-HF; Hospal Industrie) had a molecular cut-off of 10 kDa and the exchange area was limited to 2 mm with silicon glue. By means of a stereotaxic apparatus (Stoelting), the probes were implanted into the ventral hippocampus under anaesthesia (isoflurane maintenance dose: 2.0–2.5%, Iso-Vet; Dechra Veterinary Products). The head was fixed, aligned with a tooth bar, and shaved. After sagittal skin incision and mechanical cleaning of the skull bone, a circular hole of 0.8 mm diameter was drilled at the following coordinates from Bregma: AP—2.7 mm; L—3.0 mm; DV—3.8 mm. After implantation, bupivacain 0.5% Jenapharm® (mibe) was applied and the probe was fixed to the skull with glass ionomer eluting cement (Micron® i-Cem; PrevestDenPro). After surgery, the mice were placed back into their home cages in the experimental room to recover having access to food and water *ad libitum*. A minimum of 18 h was kept between probe implantation and experimental start.

Microdialysis was performed on two consecutive days starting at 09:00 ± 01:00 AM and ending in the afternoon around 2 PM. Artificial cerebrospinal fluid (aCSF) served to perfuse the probes via a microdialysis pump (KD Scientific) and had the following composition: 147 mM NaCl, 2.7 mM KCl, 1.2 mM $MgCl_2$, 1.2 mM $CaCl_2$ and 100 nM neostigmine (Acros Organics). Mice were briefly restrained for connecting the probe to the pump. Prior to sampling start, the microdialysate was discarded for 30 min. Then, the perfusion speed was set to 1 μL/min and samples were collected in microvials every 15 min. It should be noted that very low concentrations of neostigmine in the perfusate (as used in this study) cause a stabilisation of ACh release but do not prevent changes in ACh release, for example by therapeutic levels of AChE inhibitors (Chang et al., 2006; Erb et al., 2001).

On the first day, basal samples were collected while the animals stayed in their home cages for 90 min. The first two samples (collected after the start of the experiment) gave variable ACh levels and are not shown in Figures 3–6. Basal levels of ACh were calculated as averages from samples #3-#6 (30–90 min). Subsequently, mice were transferred into an open field box (45 × 32 × 20 cm). The animals were able to freely explore the new environment. A maximum of three animals was recorded in parallel in the open field. Open field boxes were cleaned carefully between animals. After 90 min, mice were placed back into their home cages. Sampling was continued for another 90 min to monitor post-interventional ACh release.

On day two, baseline levels were sampled again for 90 min in the home cage. Then, the perfusion fluid was switched to aCSF supplemented with scopolamine (1 μM) for 90 min. Finally, perfusion fluid was switched back to aCSF and samples were again collected for 90 min. After finishing microdialysis on day two, mice were anaesthetised with 5% isoflurane and decapitated. To confirm the implantation site on a random basis, some probes were perfused with the dye Fast Green (50 mM in aCSF; F7258) prior to sacrifice.

For the determination of cholinergic enzyme activities, the brain was harvested directly after decapitation. While kept on an ice-cooled petri dish, the cerebellum, the olfactory bulb and the right hemisphere were quickly removed and discarded, and the left hemisphere was weighed in a cooled potter vessel. Cold HEPES (10 mM)-sucrose (320 mM) buffer (pH 7.4) was added in a ratio of 1:10 (cortex: buffer), immediately followed by homogenisation (15 hits at 1500 rpm; Potter S, B. Braun). Aliquots of the resulting homogenate were frozen in liquid nitrogen and stored at −80°C until analysis.

2.4 | Measurement of acetylcholine

ACh was analysed using high-performance liquid chromatography (EICOM HTEC-500 HPLC + Shimadzu SIL-20AC autosampler) equipped with an electrochemical detector (ECD) sensitive to fmol amounts of ACh. The composition of the mobile phase was as follows: 50 mM $KHCO_3$, 134.3 mM EDTA-2Na (BDH) and 1.64 mM sodium decane-1-sulfonate (Alfa Aesar) in HPLC grade water, pH 8.4. Flow rate was maintained at 150 μl/min.

After the compounds of the dialysate were separated on the column, ACh was cleaved to acetate and choline by AChE in an enzyme reactor, and choline was oxidized by choline oxidase. Resulting hydrogen peroxide was detected by the ECD. External standards were used to quantify the ACh concentration of the collected samples. Peaks were integrated with the software eDAQ PowerChrom (version 2.7.12).

2.5 | Cholinergic enzyme activities

AChE enzyme activity was determined following Ellman's procedure (Ellman et al., 1961). Samples of the left hemisphere were thawed on ice and mixed with 5% Triton X-100 in PBS. Tetraisopropyl-pyrophosphoramide (iso-OMPA) diluted in Ellman buffer (Na_2HPO_4/NaH_2PO_4, pH 8.0) was used at a final concentration of 100 μM to inhibit butyrylcholinesterase. After centrifugation (12 000 *g*, 4°C, 10 min), the supernatant was used for enzyme activity and protein determination. A standard was prepared using AChE from *Electrophorus electricus*.

The activity of ChAT was determined by formation of [^{3}H]ACh from [^{3}H]acetyl-Coenzyme A (specific activity: 200 mCi/mmol; Biotrend Chemikalien) and choline chloride (Fonnum, 1969). Supernatant, as described above, was mixed with the following components (final concentrations): NaCl (0.3 M), EDTA-Na (0.02 M), Na_3PO_4 (0.05 M; pH 7.4), Triton X-100 (0.5%), neostigmine (1 mM) and choline chloride (2 mM). The mixture was incubated at 37°C for 5 min, then [^{3}H]acetyl-CoA (0.4 μCi) was added and incubated for 10 min. In ice-cooled PBS buffer, [^{3}H]ACh was extracted with 0.5% Na-tetraphenylborate in toluene/acetonitrile (85%/15%).

14714159, 2022, 2, Downloaded from https://onlinelibrary.wiley.com/doi/10.1111/jnc.15553 by Test, Wiley Online Library on [30/07/2024]. See the Terms and Conditions (https://onlinelibrary.wiley.com/terms-and-conditions) on Wiley Online Library for rules of use; OA articles are governed by the applicable Creative Commons License

Protein concentrations were determined according to Bradford (Bradford, 1976), using albumin fraction V 96% as standard.

2.6 | Data analysis and statistics

This is an exploratory study using absolute ACh values and cholinergic enzyme activities as outcomes. Both, ACh analysis and measurements of cholinergic enzyme activities, were performed by an investigator who was blinded to the study groups. Apart from that, no blinding was performed. Normal distribution was tested using the Kolmogorov–Smirnov test. No outliers were identified using the Grubbs test.

The sample size was calculated by the formula $N = 2\ SD^2 \times$ power index/delta2. Based on many years of experience, an SD of 20% was expected and a treatment effect of 25% was defined as goal of the study. The value for the power index ($\alpha = 0.05$, two-sided; ß = 0.2; 80%) was taken from the book Intuitive Statistics by Harvey Motulsky (Oxford University Press, 1995).

Basal levels of ACh (Figure 2) were analysed by one-way ANOVA with Bonferroni's post-test. Since time courses of ACh release analysed by three-way ANOVA (genotype, treatment, time) did not yield any effects with the factor genotype, we compared data for each genotype by two-way ANOVA with repeated measures (treatment vs. time; Figures 3–6). A groupwise comparison was then performed using a two-way ANOVA for selective treatments. Cholinergic enzyme activities (Figure 7) were analysed by two-way ANOVA (genotype by treatment) followed by Bonferroni's post-test. Prism 5 (GraphPad Software) was used for statistical calculation and plotting. *p*-values less than 0.05 were considered statistically significant, outliers were identified using the Grubbs test. ACh values are shown as absolute values and given as mean ± SEM. Cholinergic enzyme activities were normalised to protein and given as mean ± SEM.

3 | RESULTS

The experiment was designed so that treatments were randomised for recording days leading to single cohorts for each drug (saline/HMT/rivastigmine alone, rivastigmine + HMT; memantine, memantine + HMT). A global statistical three-way analysis of variance (treatment/genotype/time) revealed no difference between L1 and WT controls, neither at baseline nor during open field or scopolamine exposure. Also, there was no genotype by treatment interaction indicating similar levels of ACh release in response to drug administration in WT and L1 mice. We, therefore, reasoned that a more meaningful analysis should address reactions to drug exposure within each genotype separately (with the caveat that saline and HMT groups are included repeatedly in the analyses).

3.1 | Basal levels of ACh

Recorded in their home cages over 90 min, the first six samples on day one were averaged to obtain basal ACh levels (Figure 2). The control group of NMRI mice had basal ACh values in the hippocampus of 8.8 ± 1.1 nM ($N = 10$). HMT treatment more than doubled mean basal ACh levels to 22.2 ± 1.9 nM ($N = 9$; 252% of controls; $p < 0.001$). Rivastigmine also led to a significant increase in basal ACh levels to 16.0 ± 1.2 nM ($N = 8$; 182% of controls; $p < 0.05$). Notably, the combination therapy—4 weeks of rivastigmine plus 2 weeks of HMT administration—produced only a non-significant increase in

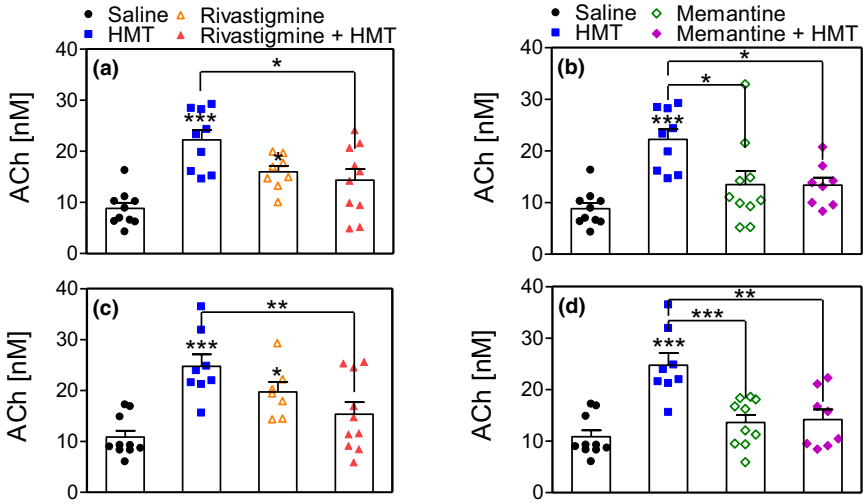

FIGURE 2 Basal ACh concentrations in the ventral hippocampus of wild-type (a + b) and tau-transgenic mice (c + d) on day one. Data are presented as means ± SEM and given as absolute values. Basal values are averages of the first six samples collected in the home cage prior to intervention on day one. Number of experiments (NMRI|L1): Saline ($N = 10|N = 10$), HMT ($N = 9|N = 8$), rivastigmine ($N = 8|N = 7$), rivastigmine + HMT ($N = 10|N = 10$), memantine ($N = 10|N = 10$) and memantine + HMT ($N = 8|N = 8$). Statistics (one-way ANOVA): (a) $F_{3,36} = 10.79$, $p < 0.001$. (b) $F_{3,36} = 8.53$, $p < 0.001$. (c) $F_{3,34} = 8.80$, $p < 0.001$. (d) $F_{3,35} = 11.95$, $p < 0.001$. Bonferroni's post-test; asterisks over the error bar consider saline group as reference: *, $p < 0.05$; **, $p < 0.01$; ***, $p < 0.001$; N = number of animals

14714159, 2022, 2, Downloaded from https://onlinelibrary.wiley.com/doi/10.1111/jnc.15553 by Test, Wiley Online Library on [30/07/2024]. See the Terms and Conditions (https://onlinelibrary.wiley.com/terms-and-conditions) on Wiley Online Library for rules of use; OA articles are governed by the applicable Creative Commons License

ACh to 14.4 ± 2.1 nM ($N = 10$; 164% of controls) (Figure 2a). In other words, pre-treatment with rivastigmine prevented the increase in basal ACh induced by HMT, but HMT also reduced the effect of rivastigmine on basal levels of ACh.

Long-term treatment with memantine had less effect on basal ACh levels than rivastigmine (Figure 2b). While HMT alone significantly increased basal ACh (see above), memantine did not (13.5 ± 2.6 nM; $N = 10$; 153% of controls; $p > 0.05$). Memantine pre-treatment blocked the ACh-enhancing effect of HMT, with ACh levels after memantine plus HMT significantly less than HMT alone (13.4 ± 1.5 nM; $N = 8$; $p < 0.05$).

The results in L1 mice, the tau-transgenic AD model, were comparable to those seen in wild-type mice (Figure 2c,d). The L1 control group had basal levels similar to wild-type mice (10.8 ± 1.3 nM; $N = 10$; t-test vs. wild-type: $p > 0.2$). HMT alone produced a highly significant increase in basal ACh values (24.8 ± 2.3 nM; $N = 8$; 230% of controls; $p < 0.001$). Treatment with rivastigmine alone also increased ACh levels significantly (19.7 ± 1.9 nM; $N = 8$; 182% of controls; $p < 0.05$), whereas the combination of rivastigmine and HMT significantly reduced ACh levels compared to HMT alone (15.3 ± 2.3 nM; $N = 10$; 142% of controls; $p < 0.05$). This again suggests an interference of by rivastigmine on the response to HMT, but also an interference by HMT on the response to rivastigmine. Memantine did not significantly changes extracellular ACh (13.6 ± 1.4 nM; $N = 10$; 126%; $p > 0.05$). When HMT was given to memantine-treated mice, ACh levels were only 14.2 ± 2.0 nM; $N = 9$; 131% of controls), a concentration that was significantly lower than HMT alone ($p < 0.01$) and not significantly different from saline-treated controls.

3.2 | ACh levels in the open field

Exposure to the open field triggered exploratory behaviour in mice and led to a clearly visible ACh release in the hippocampus as shown in Figures 3 and 4. In all treatment groups, exploration of the novel environment produced a 2- to 3-fold increase in ACh levels which returned to baseline following return to the home cage. We did not observe differences in the exploratory behaviour of either wild-type or L1 mice, and this is consistent with our previous observation that L1 mice have minimal motor deficits (Melis, Zabke, et al., 2015).

In saline-treated NMRI mice, ACh levels reached a maximum extracellular concentration of 27.3 ± 5.2 nM (equivalent to 310% of basal values) during exploration of the open field (Figure 3a). HMT treatment led to a significantly higher stimulated ACh output ($F_{1,221}$: 13.14, $p < 0.01$); a maximum value of 53.7 ± 7.6 nM was recorded (Figure 3a). However, since the basal ACh levels were higher in HMT-treated mice the relative increase was equivalent to only 252% of basal levels. ACh levels in the rivastigmine group reached a maximum 39.2 ± 6.1 nM (245% of basal levels), exceeding the absolute values for the control treatment, but remaining lower than HMT alone. Combination of rivastigmine with HMT reached a maximum ACh level of 32.7 ± 4.6 nM in the open field (227% of basal values). Total ACh release remained significantly lower than in the HMT monotherapy group ($F_{1,221}$: 8.90, $p < 0.01$) (Figure 3a).

Memantine alone did not significantly increase ACh levels (33.0 ± 5.5 nM; 244% of basal levels) (Figure 4a) when compared with saline controls. The combination of memantine plus HMT resulted in ACh values which were significantly lower than HMT alone ($F_{1,195}$: 11.50, $p < 0.01$; maximum of 33.2 ± 3.7 nM) (Figure 4a).

Comparing wild-type NMRI to L1 mice, a two-way ANOVA did not reveal any differences on day one (open field) ($F_{1,234} = 0.19$, $p > 0.5$; data from Figure 3a,b). Under open-field stimulation, 28.8 ± 4.8 nM was the peak concentration in L1 mice (267% of basal level) (Figure 3b). L1 mice showed robust responses to HMT given alone (maximum: 48.9 ± 5.1 nM; 197% of basal values; two-way ANOVA vs. saline-treated L1 mice: $F_{1,208}$: 10.35, $p < 0.01$). The effect of rivastigmine in L1 mice was similar to HMT (maximum: 47.6 ± 7.5 nM; 242% of basal values; two-way ANOVA vs. saline-treated L1 mice: $F_{1,195}$: 6.13, $p < 0.05$). However, the ACh increase under rivastigmine plus HMT was reduced to near-saline levels (maximum 34.5 ± 5.6 nM; 225% of basal values), and the time course of ACh release was not significantly different from saline-treated L1 mice (Figure 3b). L1 mice showed enhanced ACh levels under memantine monotherapy with a maximum of 39.3 ± 4.2 nM; 289% of basal levels (Figure 4b); this response was nominally higher than that seen in wild-type mice (Figure 4a), but not significantly different (see above for lack of overall genotype effect). Combined administration of memantine and HMT produced a similar time course in ACh response as in saline-treated L1 mice; ACh levels were significantly reduced relative to HMT alone ($F_{1,182}$: 11.51, $p < 0.01$; maximum 31.7 ± 2.5 nM; 223% of basal values) (Figure 4b).

3.3 | ACh levels under scopolamine

On day 2 of the experiment, perfusion of the probe with scopolamine stimulated release of ACh (Figures 5 and 6). This response is because of a block of presynaptic M_2-type muscarinic auto-receptors in hippocampus that confer negative feedback regulation of ACh release (Köppen et al., 1997), an effect which is enhanced when AChE is partially inhibited (Liu & Kato, 1994). Consequently, the infusion of scopolamine produced a five- to seven-fold stimulation of ACh release (Figures 5 and 6). As scopolamine is a highly lipophilic molecule, ACh levels return to baseline in a delayed fashion after the end of scopolamine infusion (Hartmann et al., 2010; Kopf et al., 2001). All groups of mice responded to scopolamine with strong increases of ACh release.

In saline-treated NMRI mice, ACh levels rose from 13.0 ± 2.7 nM to a maximum of 87.3 ± 24.7 nM during scopolamine perfusion (672% of basal values) (Figure 5a). NMRI mice receiving HMT or rivastigmine alone had higher basal levels than controls (27.0 ± 2.5 nM and 23.6 ± 3.6 nM, respectively) and significantly enhanced ACh levels during scopolamine perfusion ($F_{1,221}$: 10.25, $p < 0.01$ and $F_{1,208}$: 6.13, $p < 0.05$ vs. saline-treated NMRI mice, respectively). Maximum peaks of ACh were observed at 196.5 ± 33.5 nM for HMT (728%

14714159, 2022, 2, Downloaded from https://onlinelibrary.wiley.com/doi/10.1111/jnc.15553 by Test, Wiley Online Library on [30/07/2024]. See the Terms and Conditions (https://onlinelibrary.wiley.com/terms-and-conditions) on Wiley Online Library for rules of use; OA articles are governed by the applicable Creative Commons License

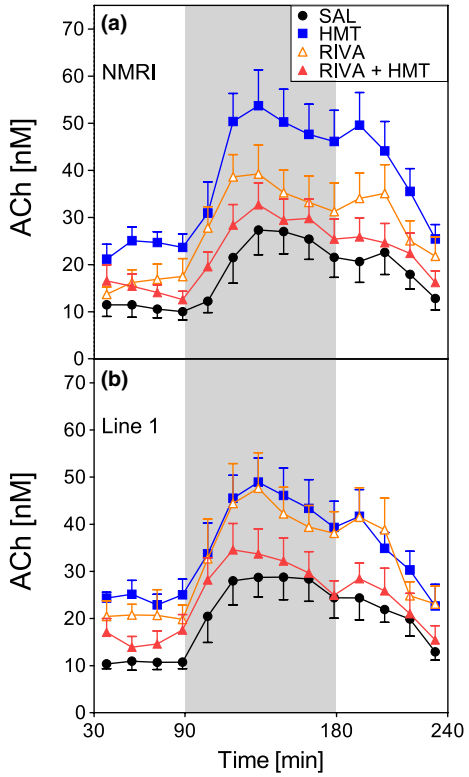

FIGURE 3 Extracellular ACh concentrations in the ventral hippocampus of wild-type (a) and line 1 (b) mice during exposure to the open field indicated by grey background. Data are presented as means ± SEM, given as absolute values and were not corrected for *in vitro*-recovery. Treatments with saline (SAL), HMT, rivastigmine (RIVA) and rivastigmine + HMT (RIVA + HMT) are shown. 30- to 90-min basal values, 90- to 180-min behavioural activation (exposure to novel environment, "open field"), 180 to 240 min home cage. Number of experiments (NMRI|L1): Saline (N = 10|10), HMT (N = 9|8), rivastigmine (N = 8|7), rivastigmine + HMT (N = 10|10). Statistics (two-way ANOVA): (a) Treatment $F_{3,429} = 5.56$, $p < 0.01$. (b) Treatment $F_{3,403} = 3.81$, $p < 0.05$. Significant differences were found when directly comparing the following ACh curves: (a) Saline versus HMT, $F_{1,221}$: 13.14, $p < 0.01$; HMT versus rivastigmine + HMT, $F_{1,221}$: 8.90, $p < 0.01$. (b) Saline versus HMT, $F_{1,208}$: 10.35, $p < 0.01$; saline versus rivastigmine, $F_{1,195}$: 6.13, $p < 0.05$; N = number of animals

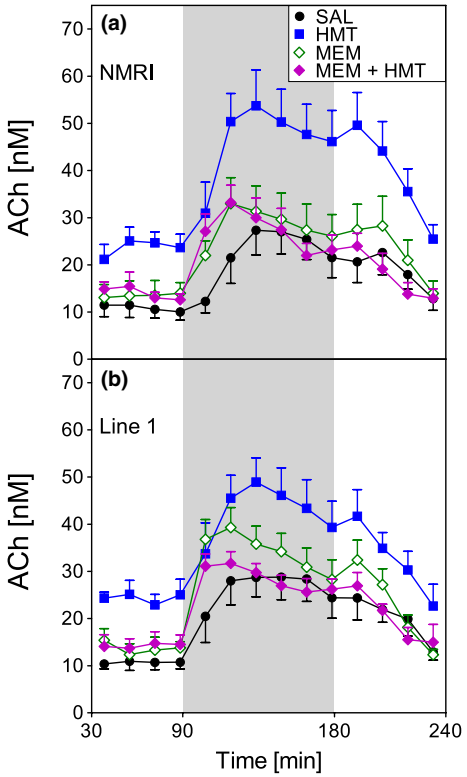

FIGURE 4 Extracellular ACh concentrations in the ventral hippocampus of wild-type (a) and line 1 (b) mice during exposure to the open field indicated by grey background. Data are presented as means ± SEM, given as absolute values and were not corrected for *in vitro* recovery. Treatments with saline (SAL), HMT, memantine (MEM) and memantine + HMT (MEM + HMT) are shown. 30- to 90-min basal values, 90- to 180-min behavioural activation (exposure to novel environment, "open field"), 180 to 240 min home cage. Number of experiments (NMRI|L1): saline (N = 10|10), HMT (N = 9|8), memantine (N = 10|10) and memantine + HMT (N = 8|8). Statistics (two-way ANOVA for treatment as variable): (a) Treatment $F_{3,429} = 5.89$, $p < 0.01$. (b) Treatment $F_{3,416} = 4.87$, $p < 0.01$. Significant differences were found when directly comparing the following ACh curves: (a) Saline versus HMT, $F_{1,221}$: 13.14, $p < 0.01$; HMT versus memantine + HMT, $F_{1,195}$: 11.50, $p < 0.01$. (b) Saline versus HMT, $F_{1,208}$: 10.35, $p < 0.01$; HMT versus memantine + HMT, $F_{1,182}$: 11.51, $p < 0.01$; N = number of animals

of basal levels) and 167.9 ± 35.3 nM for rivastigmine (711% of basal values) (Figure 5a). Again, the combination of both drugs produced low basal ACh levels (15.8 ± 2.3 nM), with a lower maximum release (70.6 ± 20.5 nM; 447% of basal values), and a significant decrease compared to either treatment alone (Figure 5a). Memantine-treated NMRI mice had a maximum of 119.6 ± 19.0 nM (595% of basal values) (Figure 6a). The combination of memantine and HMT produced basal levels of 16.8 ± 1.8 nM and a maximum ACh release of 95.5 ± 13.8 nM (568% of basal values); these values were not significantly different from those of saline-treated NMRI mice (Figure 6a).

Tau-transgenic L1 mice also responded with strong increases of ACh levels following scopolamine infusion, albeit at a somewhat lower level than NMRI mice. Although the maximum ACh level in saline-treated L1 mice was lower by 20% than in wild-type mice, statistical analysis of the ACh time courses showed no significance (two-way ANOVA: $F_{1,234} < 0.001$, $p > 0.9$). Scopolamine treatment in L1 mice raised basal ACh levels from 15.0 ± 1.8 nM to a maximum of 69.3 ± 15.9 nM (462% of basal values) (Figure 5b). Following HMT treatment alone, extracellular ACh was enhanced significantly versus saline-treated L1 mice ($F_{1,195}$: 16.51, $p < 0.01$); it increased from 30.5 ± 2.7 nM to 139.2 ± 24.8 nM (456% of basal values). A significant increase versus saline-treated L1 mice was also observed in the rivastigmine group ($F_{1,195}$: 7.12, $p < 0.05$): ACh basal levels started at 23.5 ± 3.9 nM and reached a maximum of 129.5 ± 19.2 nM (551% of basal values). Rivastigmine in combination with HMT produced basal ACh levels of 20.1 ± 2.2 nM, which increased to 108.1 ± 20.6 nM (538% of basal values) following scopolamine (Figure 5b). Interestingly, memantine alone was also able to

14714159, 2022, 2, Downloaded from https://onlinelibrary.wiley.com/doi/10.1111/jnc.15553 by Test, Wiley Online Library on [30/07/2024]. See the Terms and Conditions (https://onlinelibrary.wiley.com/terms-and-conditions) on Wiley Online Library for rules of use; OA articles are governed by the applicable Creative Commons License

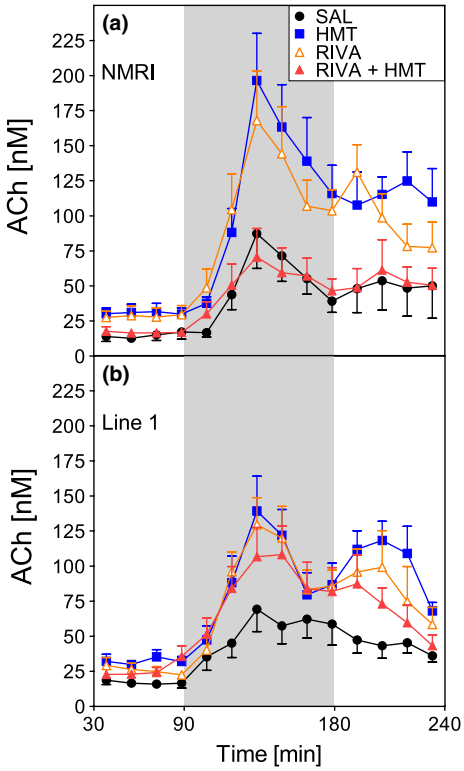

FIGURE 5 Extracellular ACh concentrations in the ventral hippocampus of wild-type (a) and line 1 (b) mice during scopolamine perfusion indicated by grey background. Data are presented as means ± SEM, given as absolute values and were not corrected for *in vitro* recovery. Treatments with saline (SAL), HMT, rivastigmine (RIVA) and rivastigmine + HMT (RIVA + HMT) are shown. 30- to 90-min aCSF perfusion, 90- to 180-min perfusion with 1 μM scopolamine, 180- to 240-min perfusion with aCSF. Number of experiments (NMRI|L1): saline (N = 10|10), HMT (N = 9|7), rivastigmine (N = 8|7), rivastigmine + HMT (N = 10|10). Statistics (two-way ANOVA for treatment as variable): (a) Treatment $F_{3,429} = 5.77$, $p < 0.01$. (b) Treatment $F_{3,390} = 3.87$, $p < 0.05$. Significant differences were found when directly comparing the following ACh curves: (a) Saline versus HMT, $F_{1,221}$: 10.25, $p < 0.01$; saline versus rivastigmine, $F_{1,208}$: 6.13, $p < 0.05$; rivastigmine versus rivastigmine + HMT, $F_{1,208} = 6.64$, $p < 0.05$; HMT versus rivastigmine + HMT, $F_{1,221}$: 11.19, $p < 0.01$. (b) Saline versus HMT, $F_{1,195}$: 16.51, $p < 0.01$; saline versus rivastigmine, $F_{1,195}$: 7.12, $p < 0.05$; N = number of animals

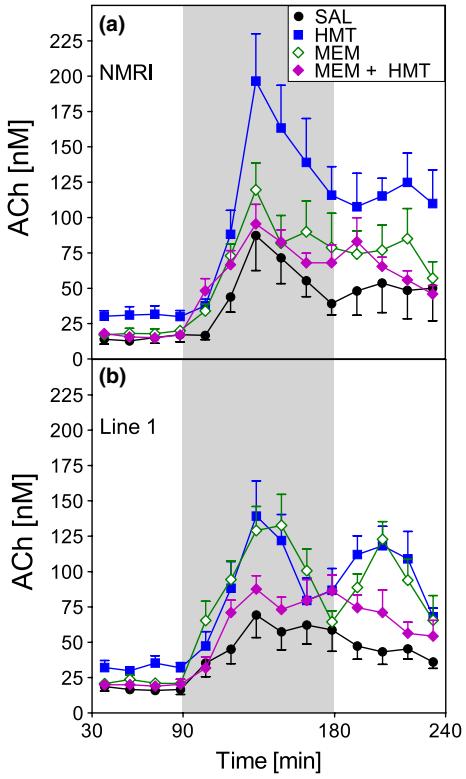

FIGURE 6 Extracellular ACh concentrations in the ventral hippocampus of wild-type (a) and line 1 (b) mice during scopolamine perfusion indicated by grey background. Data are presented as means ± SEM, given as absolute values and were not corrected for *in vitro* recovery. (a) Treatments with saline (SAL), HMT, memantine (MEM) and memantine + HMT (MEM + HMT) are shown. 30- to 90-min aCSF perfusion, 90- to 180-min perfusion with 1 μM scopolamine, 180- to 240-min perfusion with aCSF. Number of experiments (NMRI|L1): saline (N = 10|10), HMT (N = 9|7), memantine (N = 10|9) and memantine + HMT (N = 8|7). Statistics (two-way ANOVA for treatment as variable): (A) Treatment $F_{3,429} = 4.85$, $p < 0.01$. (b) Treatment $F_{3,377} = 8.17$, $p < 0.001$. Significant differences were found when directly comparing the following ACh curves: (a) Saline versus HMT, $F_{1,221}$: 10.25, $p < 0.01$; HMT versus memantine + HMT, $F_{1,195}$: 8.69, $p < 0.01$. (b) Saline versus HMT, $F_{1,195}$: 16.51, $p < 0.01$; saline versus memantine, $F_{1,221}$: 12.45, $p < 0.01$; HMT versus memantine + HMT, $F_{1,156}$: 10.42, $p < 0.01$; N = number of animals

increase ACh release significantly in L1 mice ($F_{1,221}$: 12.45, $p < 0.01$), starting from 21.9 ± 2.2 nM at baseline to a maximum ACh value of 132.6 ± 22.0 nM (605% of basal values) following scopolamine. This increase is comparable to the increase produced by rivastigmine (Figure 5b) or HMT (Figure 6b). By contrast, combination of memantine with HMT produced a scopolamine response which was significantly lower than HMT alone ($F_{1,156}$: 10.42, $p < 0.01$), starting at 20.1 ± 2.5 nM and reaching a maximum of 87.6 ± 9.6 nM (436% of basal values) (Figure 6b). It follows that treatment-dependent effects on basal ACh levels are largely identical in L1 mice and NMRI mice, whereas the relative increase induced by scopolamine is somewhat lower in transgenic L1 mice.

3.4 | Cholinergic enzyme activities

AChE activities and responses to drug treatments were similar in both strains (Figure 7a). While AChE activity was slightly lower in NMRI mice (408.1 ± 14.2 mU/mg) than in L1 mice (456.5 ± 18.6 mU/mg; t-test: $p > 0.4$), significant changes in either strain were seen only in animals receiving rivastigmine. In wild-type animals, rivastigmine significantly decreased AChE activity when given alone (to 302.1 ± 14.5 mU/mg; 74% of controls) or in combination with HMT (to 330.0 ± 20.4 mU/mg; 81% of controls). L1 mice responded similarly, showing decreased AChE activity after rivastigmine alone (326.6 ± 20.6 mU/mg; 72% of controls) and after the rivastigmine/HMT combination (373.6 ± 15; 82% of controls). AChE

14714159, 2022, 2, Downloaded from https://onlinelibrary.wiley.com/doi/10.1111/jnc.15553 by Test, Wiley Online Library on [30/07/2024]. See the Terms and Conditions (https://onlinelibrary.wiley.com/terms-and-conditions) on Wiley Online Library for rules of use; OA articles are governed by the applicable Creative Commons License

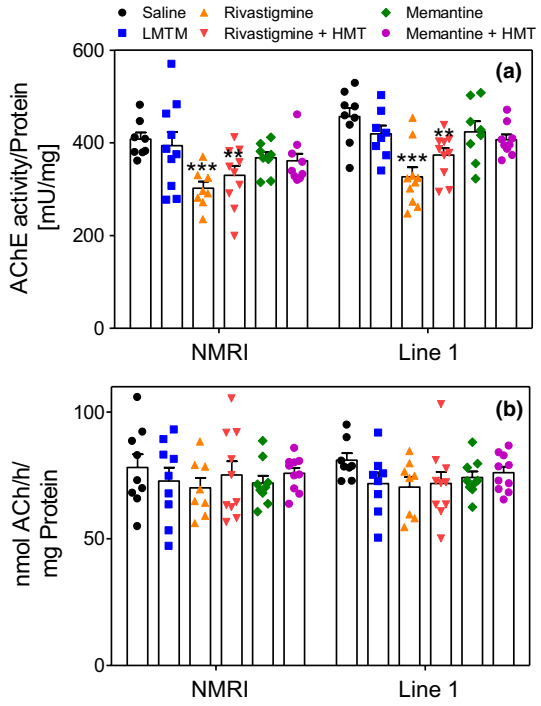

FIGURE 7 Activity of acetylcholinesterase (a) and choline acetyltransferase (b). Data are presented as means ± SEM, normalised to protein. Abbreviations are used for saline (SAL), rivastigmine (RIVA) and memantine (MEM). (a) Number of experiments (NMRI|L1): saline ($N = 8|N = 9$), HMT ($N = 10|N = 8$), rivastigmine ($N = 8|N = 10$), rivastigmine + HMT ($N = 10|N = 10$), memantine ($N = 8|N = 8$) and memantine + HMT ($N = 9|N = 9$). Statistics (two-way ANOVA): Treatment $F_{5,95} = 9.68$, $p < 0.001$. (b) Number of experiments (NMRI|L1): saline ($N = 9|N = 8$), HMT ($N = 9|N = 8$), rivastigmine ($N = 8|N = 8$), rivastigmine + HMT ($N = 10|N = 10$), memantine ($N = 9|N = 9$) and memantine + HMT ($N = 10|N = 10$). Statistics (two-way ANOVA): Treatment ns. Bonferroni's post-test; asterisks over the error bar consider saline group as reference: $^{*}p < 0.05$; $^{**}p < 0.01$; $^{***}p < 0.001$; N = number of animals

activity remained unchanged following HMT given alone (NMRI: 394 ± 29.7 mU/mg; 97% of controls; L1: 419.3 ± 18.2 mU/mg; 92% of controls; two-way ANOVA: $F_{1,31} = 1.3$, $p > 0.2$). Memantine did not influence AChE activity either in the strains or under different treatment conditions (Figure 7a).

The activity of ChAT, the enzyme that synthesises ACh, was 78.1 ± 5.2 nmol ACh/h/mg in NMRI mice and 81 ± 2.8 nmol ACh/h/mg in L1 mice (Figure 7b). Neither treatment caused significant changes in the enzyme activity in cortico-hippocampal homogenates indicating that the potential to synthesise ACh in mouse brains was unchanged.

4 | DISCUSSION

The present study investigated central cholinergic systems in two mouse lines using microdialysis to quantify extracellular levels of ACh in hippocampus. As shown previously (Hartmann et al., 2010; Kopf et al., 2001), exploration of a novel environment causes an increase in hippocampal ACh levels by 2- to 3-fold, whereas pharmacological stimulation (by infusion of scopolamine) causes a strong, 5- to 7-fold increase in ACh (Hartmann et al., 2010; Kopf et al., 2001). L1 mice that express a truncated tau protein and develop tau pathology had similar hippocampal ACh levels as controls and were also able to enhance cholinergic tone during behavioural activation in the open field. However, their ACh levels remained somewhat lower during pharmacological stimulation which may indicate a slightly reduced cholinergic capacity during global neuronal stimulation. This reduction in central cholinergic tone is probably age-dependent and is reminiscent of a more pronounced central cholinergic dysfunction in aged P301L tau-transgenic mice that we investigated previously (Stein et al., 2019).

The focus of the present study was to investigate cholinergic actions of HMT, a novel anti-dementia drug that yielded beneficial results in drug-naïve patients in a clinical study of dementia (Gauthier et al., 2016; Schelter et al., 2019; Wilcock et al., 2018). Notably, HMT had less benefit when patients had been pre-treated with cholinesterase inhibitors and/or memantine. The main objective of the present study was, therefore, to determine whether a similar negative interaction occurs in wild-type mice and in a mouse model of Alzheimer´s disease, the tau-transgenic L1 mouse, using cholinergic activity as the outcome parameter. We used a drug treatment schedule in which we treated either with rivastigmine (0.5 mg/kg/day) or memantine (1 mg/kg/day) given by chronic systemic infusion, before HMT (5 mg/kg/d) was added for a further 2 weeks by oral gavage. The study was carried out in 6- to 8-month-old mice because cognitive deficits were already visible in L1 mice at this age (Melis, Zabke, et al., 2015).

In our hands, HMT had robust pro-cholinergic actions because it increased hippocampal ACh levels more strongly than the AChE inhibitor rivastigmine. The most interesting finding of the present study is that a negative interaction between HMT and rivastigmine or memantine, respectively, was observed in the tau-transgenic mouse model of AD. Administration of HMT in combination with either rivastigmine or memantine had less effect on ACh levels than HMT alone, and this surprising interaction was seen both in wild-type NMRI and in tau-transgenic L1 mice. Our finding in murine models exactly matches the picture seen in the completed clinical trials, that is pre-treatment with two established anti-dementia drugs reduced the beneficial clinical effects of LMT. In mice, HMT given alone caused a highly significant rise of ACh levels and rivastigmine (at the chosen dose) a more limited increase, while memantine only affected the ACh response in L1 mice. However, it should be noted that there was no overall genotype or treatment by genotype interactions, suggesting that the treatment effects might be similar in both wild-type and L1 mice. Intriguingly, the pronounced effect of HMT alone on ACh levels during exploration in the open field was completely prevented by rivastigmine or memantine co-administration in both strains (Figures 3 and 4). At the same time, the lesser increase in ACh levels induced by rivastigmine was also blocked by the combination with HMT. This

14714159, 2022, 2, Downloaded from https://onlinelibrary.wiley.com/doi/10.1111/jnc.15553 by Test, Wiley Online Library on [30/07/2024]. See the Terms and Conditions (https://onlinelibrary.wiley.com/terms-and-conditions) on Wiley Online Library for rules of use; OA articles are governed by the applicable Creative Commons License

is surprising and remains unexplained mechanistically. What appears certain is that while rivastigmine inhibited AChE, the strong increases in ACh levels after long-term HMT treatment are not the result of the same mechanism of action. Our preliminary evidence seems to suggest an indirect action via glutamatergic or other neurotransmitters (Cranston et al., in preparation), or more globally through actions on mitochondrial functions (see below) or synaptic protein levels and release mechanisms (Riedel et al., 2020). These alternative mechanisms would also be consistent with enhanced basal levels of ACh in hippocampus under HMT treatment in both genotypes despite a reduction in ChAT-positive neuronal labelling in the basal forebrain and AChE levels in cortex and hippocampus of L1 mice (Cranston et al., 2020).

Upon scopolamine infusion, disinhibition because of the blockade of hippocampal M_2-autoreceptors produced ACh increases of up to 5- to 7-fold (Figures 5 and 6). It is notable that NMRI and L1 mice had comparable ACh values in the control condition. L1 mice appeared to have a lower cholinergic capacity under maximum stimulation (during perfusion with scopolamine), but again, the lack of overall genotype and genotype/treatment differences should be born in mind. During scopolamine perfusion, extracellular ACh concentrations reached 160–200 nM while maximum levels in L1 mice ranged lower (between 130 and 140 nM). This reduced ACh release was not accompanied by an overall reduction in ChAT activity in L1 mice. However, a recent study reported a reduction in ChAT-positive neuronal labelling in the basal forebrain of L1 mice (Cranston et al., 2020). While ChAT is not rate-limiting for ACh synthesis under basal conditions (Brandon et al., 2004), the high demand for ACh synthesis induced by scopolamine perfusion is consistent with an impairment in cholinergic function resulting from tau aggregation pathology.

The scopolamine response was strong in rivastigmine-treated wild-type mice, an observation that is likely because of the higher feedback inhibition during rivastigmine-induced AChE inhibition which enhanced the efficiency of scopolamine (Liu & Kato, 1994). L1 animals showed this effect to a lesser extent which might point to an altered presynaptic M_2-receptor expression, as described before in post-mortem studies of AD patients (Mash et al., 1985), or to a diminished receptor response (Mohr et al., 2015). The fact that both strains respond to rivastigmine with enhanced ACh release, but only transgenic mice responded to the glutamate receptor antagonist memantine, suggests altered glutamatergic transmission in L1 animals, as reported previously (Riedel et al., 2020). Of note, interactions between tau pathology and cholinergic and glutamatergic signalling are highly complex, limiting the extent to which these can be elucidated at a cellular level using microdialysis.

The explanation for the negative interaction between HMT and symptomatic AD drugs remains to be established. It should be noted that MTC, which delivers the oxidised form of the methylthionium moiety, needs to be converted to HMT to permit efficient absorption and distribution to the brain (Baddeley et al., 2015). MTC inhibits AChE in micromolar concentrations in vitro (Augustinsson, 1950; Pfaffendorf et al., 1997). The present data clearly demonstrate that HMT (at the dose given) does not act as an AChE inhibitor *in vivo* since its action on ACh was counteracted by rivastigmine (Figures 3 and 5). This conclusion was corroborated by measurement of AChE activity in brain homogenates where HMT had no influence (Figure 7a). We conclude that the enhanced ACh levels measured after HMT alone cannot be explained by changes in the rate of enzymatic hydrolysis or of ACh synthesis (Figure 7b). Rather, enhanced cholinergic tone must be because of an effect of the drug on other neuronal systems. Although the mechanism of the HMT-ACh interaction remains elusive, our data suggest that it is independent of cortical tau load since both HMT-mediated effects and their attenuation by pre-treatment with symptomatic AD drugs were similar in wild-type and in L1 mice.

As MTC is converted to HMT *in vivo* (Baddeley et al., 2015), several of the effects reported for MTC (Oz et al., 2011; Schirmer et al., 2011) may be relevant for HMT. Both MTC and HMT are effective inhibitors of tau aggregation *in vitro* (Akoury et al., 2013; Harrington et al., 2015; Wischik et al., 1996). Both MTC and HMT reduced the limbic load of tau in L1 mice (Melis, Magbagbeolu, et al., 2015), and HMT was found to be active in a mouse model of synucleinopathy (Schwab et al., 2017). The methylthionium moiety has a redox potential close to zero and so is able to act as a supplementary electron carrier in the mitochondrial electron transport chain (Tretter et al., 2014) and has been shown to improve respiration in isolated mitochondria (Atamna et al., 2008; Harpey et al., 1986; Visarius et al., 1997). Therefore, one of the possible pathway whereby HMT may influence cholinergic neurons is by enhancing metabolism in synaptic mitochondria, a hypothesis that is a focus of our ongoing studies.

An alternative explanation may be an effect on neuronal systems that influence ACh release in hippocampus (Dazzi et al., 1995). Both GABA and glutamate are prominent regulators of hippocampal ACh release, either via direct input from the basal forebrain or through interneurons (Freund & Antal, 1988; Giovannini et al., 1994), and an effect of HMT on GABAergic or glutamatergic mechanisms has been described recently (Riedel et al., 2020). It follows that the action of HMT on the cholinergic systems may well involve interactions with a variety of targets.

In summary, HMT enhances cholinergic activity independently of AChE inhibition. Our findings demonstrate, in both a mouse model of AD and in wild-type mice, that the effects of HMT on cholinergic function are inhibited by pre-treatment with both a prototypic AChE inhibitor and a glutamate receptor modulator. Therefore, the interference by commonly used AD symptomatic drugs in the treatment effects of HMT observed in the AD clinical trials can be reproduced in mouse models. The results we report provide strong support for underlying neuropharmacological mechanisms as the explanation of the interaction. Therefore, clinically relevant interactions can occur in clinical trials even though HMT and symptomatic AD drugs have different mechanisms of action. This has broad-reaching implications for the design of clinical trials of novel disease-modifying drugs in AD.

ACKNOWLEDGEMENTS

The present study was carried out with funds supplied by TauRx Therapeutic Ltd. We are grateful to Helene Lau for assistance with

14714159, 2022, 2, Downloaded from https://onlinelibrary.wiley.com/doi/10.1111/jnc.15553 by Test, Wiley Online Library on [30/07/2024]. See the Terms and Conditions (https://onlinelibrary.wiley.com/terms-and-conditions) on Wiley Online Library for rules of use; OA articles are governed by the applicable Creative Commons License

the analytical determinations. Open access funding enabled and organized by ProjektDEAL.

All experiments were conducted in compliance with the ARRIVE guidelines.

CONFLICT OF INTEREST

C.R.H and C.M.W. are employed by TauRx Therapeutic Ltd. C.K., G.R. and J.K. have received funding from TauRx Therapeutic Ltd.

AUTHOR CONTRIBUTION

C.K. performed the experimental work. G.R. and J.K. planned the study and supervised the work. C.R.H. and C.M.W. provided input at the planning stage, secured funding contributed to the interpretation of the data and to the final manuscript. C.K., G.R. and J.K. wrote the manuscript. All authors reviewed the final submission.

DATA AVAILABILITY STATEMENT

The data that support the findings of this study are available from the corresponding author upon reasonable request.

ORCID

Jochen Klein https://orcid.org/0000-0001-6971-3381

REFERENCES

Akoury, E., Pickhardt, M., Gajda, M., Biernat, J., Mandelkow, E., & Zweckstetter, M. (2013). Mechanistic basis of phenothiazine-driven inhibition of Tau aggregation. *Angewandte Chemie (International Ed. in English)*, 52, 3511–3515. https://doi.org/10.1002/anie.201208290

Anderson, R. M., Hadjichrysanthou, C., Evans, S., & Wong, M. M. (2017). Why do so many clinical trials of therapies for Alzheimer's disease fail? *The Lancet*, 390, 2327–2329. https://doi.org/10.1016/S0140-6736(17)32399-1

Arendt, T., Holzer, M., Gertz, H. J., & Brückner, M. K. (1999). Cortical load of PHF-tau in Alzheimer's disease is correlated to cholinergic dysfunction. *Journal of Neural Transmission*, 106, 513–523. https://doi.org/10.1007/s007020050175

Atamna, H., Nguyen, A., Schultz, C., Boyle, K., Newberry, J., Kato, H., & Ames, B. N. (2008). Methylene blue delays cellular senescence and enhances key mitochondrial biochemical pathways. *The FASEB Journal*, 22, 703–712. https://doi.org/10.1096/fj.07-9610com

Augustinsson, K.-B. (1950). Methylene blue as an inhibitor of acetylcholine-esterase. *Acta Chemica Scandinavica*, 4, 536–542.

Baddeley, T. C., McCaffrey, J., Storey, J. M. D., Cheung, J. K. S., Melis, V., Horsley, D., Harrington, C. R., & Wischik, C. M. (2015). Complex disposition of methylthioninium redox forms determines efficacy in tau aggregation inhibitor therapy for Alzheimer's disease. *Journal of Pharmacology and Experimental Therapeutics*, 352, 110–118. https://doi.org/10.1124/jpet.114.219352

Blanco-Silvente, L., Capellà, D., Garre-Olmo, J., Vilalta-Franch, J., & Castells, X. (2018). Predictors of discontinuation, efficacy, and safety of memantine treatment for Alzheimer's disease: meta-analysis and meta-regression of 18 randomized clinical trials involving 5004 patients. *BMC Geriatr*, 18, 168. https://doi.org/10.1186/s12877-018-0857-5

Bonanno, G., Ruelle, A., Andrioli, G. C., & Raiteri, M. (1991). Cholinergic nerve terminals of human cerebral cortex possess a GABA transporter whose activation induces release of acetylcholine. *Brain Research*, 539, 191–195. https://doi.org/10.1016/0006-8993(91)91620-G

Braak, H., & Braak, E. (1991). Neuropathological stageing of Alzheimer-related changes. *Acta Neuropathologica*, 82, 239–259. https://doi.org/10.1007/BF00308809

Braak, H., & Del Tredici, K. (2013). Reply: The early pathological process in sporadic Alzheimer's disease. *Acta Neuropathologica*, 126, 615–618. https://doi.org/10.1007/s00401-013-1170-1

Bradford, M. M. (1976). A rapid and sensitive method for the quantitation of microgram quantities of protein utilizing the principle of protein-dye binding. *Analytical Biochemistry*, 72, 248–254. https://doi.org/10.1016/0003-2697(76)90527-3

Brandon, E. P., Mellott, T., Pizzo, D. P., Coufal, N., D'Amour, K. A., Gobeske, K., Lortie, M., López-Coviella, I., Berse, B., Thal, L. J., Gage, F. H., & Blusztajn, J. K. (2004). Choline transporter 1 maintains cholinergic function in choline acetyltransferase haploinsufficiency. *Journal of Neuroscience*, 24, 5459–5466. https://doi.org/10.1523/JNEUROSCI.1106-04.2004

Chang, Q., Savage, L. M., & Gold, P. E. (2006). Microdialysis measures of functional increases in ACh release in the hippocampus with and without inclusion of acetylcholinesterase inhibitors in the perfusate. *Journal of Neurochemistry*, 97, 697–706. https://doi.org/10.1111/j.1471-4159.2006.03765.x

Cranston, A. L., Wysocka, A., Steczkowska, M., Zadrożny, M., Palasz, E., Harrington, C. R., Theuring, F., Wischik, C. M., Riedel, G., & Niewiadomska, G. (2020). Cholinergic and inflammatory phenotypes in transgenic tau mouse models of Alzheimer's disease and frontotemporal lobar degeneration. *Brain Commun*, 2, fcaa033. https://doi.org/10.1093/braincomms/fcaa033

Cummings, J. L., Morstorf, T., & Zhong, K. (2014). Alzheimer ' s disease drug-development pipeline: few candidates, frequent failures. *Alzheimer's Research and Therapy*, 6(4), 37. https://doi.org/10.1186/alzrt269

Dazzi, L., Motzo, C., Imperato, A., Serra, M., Gessa, G. L., & Biggio, G. (1995). Modulation of basal and stress-induced release of acetylcholine and dopamine in rat brain by abecarnil and imidazenil, two anxioselective gamma-aminobutyric acidA receptor modulators. *Journal of Pharmacology and Experimental Therapeutics*, 273, 241–247.

Deiana, S., Harrington, C. R., Wischik, C. M., & Riedel, G. (2009). Methylthioninium chloride reverses cognitive deficits induced by scopolamine: comparison with rivastigmine. *Psychopharmacology (Berl)*, 202, 53–65. https://doi.org/10.1007/s00213-008-1394-2

Ellman, G. L., Courtney, K., Andres, V., & Featherstone, R. M. (1961). A new and rapid colorimetric determination of acetylcholinesterase activity. *Biochemical Pharmacology*, 7, 88–95. https://doi.org/10.1016/0006-2952(61)90145-9

Erb, C., Troost, J., Kopf, S., Schmitt, U., Löffelholz, K., Soreq, H., & Klein, J. (2001). Compensatory mechanisms enhance hippocampal acetylcholine release in transgenic mice expressing human acetylcholinesterase. *Journal of Neurochemistry*, 77, 638–646. https://doi.org/10.1046/j.1471-4159.2001.00287.x

Fonnum, F. (1969). Radiochemical micro assays for the determination of choline acetyltransferase and acetylcholinesterase activities. *The Biochemical Journal*, 115, 465–472. https://doi.org/10.1042/bj1150465

Freund, T. F., & Antal, M. (1988). GABA-containing neurons in the septum control inhibitory interneurons in the hippocampus. *Nature*, 336, 170–173. https://doi.org/10.1038/336170a0

Gauthier, S., Feldman, H. H., Schneider, L. S., Wilcock, G. K., Frisoni, G. B., Hardlund, J. H., Moebius, H. J., Bentham, P., Kook, K. A., Wischik, D. J., Schelter, B. O., Davis, C. S., Staff, R. T., Bracoud, L., Shamsi, K., Storey, J. M. D., Harrington, C. R., & Wischik, C. M. (2016). Efficacy and safety of tau-aggregation inhibitor therapy in patients with mild or moderate Alzheimer's disease: A randomised, controlled, double-blind, parallel-arm, phase 3 trial.

14714159, 2022, 2, Downloaded from https://onlinelibrary.wiley.com/doi/10.1111/jnc.15553 by Test, Wiley Online Library on [30/07/2024]. See the Terms and Conditions (https://onlinelibrary.wiley.com/terms-and-conditions) on Wiley Online Library for rules of use; OA articles are governed by the applicable Creative Commons License

The Lancet, 388, 2873–2884. https://doi.org/10.1016/S0140-6736(16)31275-2

Geula, C., Nagykery, N., Nicholas, A., & Wu, C.-K. (2008). Cholinergic neuronal and axonal abnormalities are present early in aging and in Alzheimer disease. *Journal of Neuropathology and Experimental Neurology*, 67, 309–318. https://doi.org/10.1097/NEN.0b013e31816a1df3

Ginsberg, S. D., Che, S., Counts, S. E., & Mufson, E. J. (2006). Shift in the ratio of three-repeat tau and four-repeat tau mRNAs in individual cholinergic basal forebrain neurons in mild cognitive impairment and Alzheimer's disease. *Journal of Neurochemistry*, 96, 1401–1408. https://doi.org/10.1111/j.1471-4159.2005.03641.x

Giovannini, M. G., Mutolo, D., Bianchi, L., Michelassi, A., & Pepeu, G. (1994). NMDA receptor antagonists decrease GABA outflow from the septum and increase acetylcholine outflow from the hippocampus: A microdialysis study. *Journal of Neuroscience*, 14, 1358–1365. https://doi.org/10.1523/JNEUROSCI.14-03-01358.1994

Hampel, H., Mesulam, M.-M., Cuello, A. C., Farlow, M. R., Giacobini, E., Grossberg, G. T., Khachaturian, A. S., Vergallo, A., Cavedo, E., Snyder, P. J., & Khachaturian, Z. S. (2018). The cholinergic system in the pathophysiology and treatment of Alzheimer's disease. *Brain*, 141, 1917–1933. https://doi.org/10.1093/brain/awy132

Harpey, J.-P., Charpentier, C., & Coudé, M. (1986). Methylene-blue for riboflavin-unresponsive glutaricaciduria type II. *The Lancet*, 327, 391. https://doi.org/10.1016/S0140-6736(86)92361-5

Harrington, C. R., Storey, J. M. D., Clunas, S., Harrington, K. A., Horsley, D., Ishaq, A., Kemp, S. J., Larch, C. P., Marshall, C., Nicoll, S. L., Rickard, J. E., Simpson, M., Sinclair, J. P., Storey, L. J., & Wischik, C. M. (2015). Cellular models of aggregation-dependent template-directed proteolysis to characterize tau aggregation inhibitors for treatment of Alzheimer disease. *Journal of Biological Chemistry*, 290, 10862–10875. https://doi.org/10.1074/jbc.M114.616029

Hartmann, J., Kiewert, C., & Klein, J. (2010). Neurotransmitters and energy metabolites in amyloid-bearing APP(SWE)xPSEN1dE9 mouse brain. *Journal of Pharmacology and Experimental Therapeutics*, 332, 364–370. https://doi.org/10.1124/jpet.109.161091

Hasselmo, M. E. (2006). The role of acetylcholine in learning and memory. *Current Opinion in Neurobiology*, 16, 710–715. https://doi.org/10.1016/j.conb.2006.09.002

Kaduszkiewicz, H., Zimmermann, T., Beck-Bornholdt, H.-P., & van den Bussche, H. (2005). Cholinesterase inhibitors for patients with Alzheimer's disease: systematic review of randomised clinical trials. *British Medical Journal*, 331, 321–327. https://doi.org/10.1136/bmj.331.7512.321

Kopf, S. R., Buchholzer, M. L., Hilgert, M., Löffelholz, K., & Klein, J. (2001). Glucose plus choline improve passive avoidance behaviour and increase hippocampal acetylcholine release in mice. *Neuroscience*, 103, 365–371. https://doi.org/10.1016/s0306-4522(01)00007-0

Köppen, A., Klein, J., Erb, C., & Löffelholz, K. (1997). Acetylcholine release and choline availability in rat hippocampus: Effects of exogenous choline and nicotinamide. *Journal of Pharmacology and Experimental Therapeutics*, 282, 1139–1145.

Lietsche, J., Gorka, J., Hardt, S., Karas, M., & Klein, J. (2014). Self-built microdialysis probes with improved recoveries of ATP and neuropeptides. *Journal of Neuroscience Methods*, 237, 1–8. https://doi.org/10.1016/j.jneumeth.2014.08.015

Liu, J. K., & Kato, T. (1994). Effect of physostigmine on relative acetylcholine output induced by systemic treatment with scopolamine in in vivo microdialysis of rat frontal cortex. *Neurochemistry International*, 24, 589–596. https://doi.org/10.1016/0197-0186(94)90012-4

Mash, D. C., Flynn, D. D., & Potter, L. T. (1985). Loss of M2 muscarine receptors in the cerebral cortex in Alzheimer's disease and experimental cholinergic denervation. *Science*, 228, 1115–1117. https://doi.org/10.1126/science.3992249

McShane, R., & Schneider, L. S. (2005). Meta-analysis of memantine: Summary and commentary on the Cochrane Collaboration's systematic review. *Alzheimer's and Dementia: the Journal of the Alzheimer's Association*, 1, 67–71. https://doi.org/10.1016/j.jalz.2005.06.025

Melis, V., Magbagbeolu, M., Rickard, J. E., Horsley, D., Davidson, K., Harrington, K. A., Goatman, K., Goatman, E. A., Deiana, S., Close, S. P., Zabke, C., Stamer, K., Dietze, S., Schwab, K., Storey, J. M. D., Harrington, C. R., Wischik, C. M., Theuring, F., & Riedel, G. (2015). Effects of oxidized and reduced forms of methylthioninium in two transgenic mouse tauopathy models. *Behavioural Pharmacology*, 26, 353–368. https://doi.org/10.1097/FBP.0000000000000133

Melis, V., Zabke, C., Stamer, K., Magbagbeolu, M., Schwab, K., Marschall, P., Veh, R. W., Bachmann, S., Deiana, S., Moreau, P.-H., Davidson, K., Harrington, K. A., Rickard, J. E., Horsley, D., Garman, R., Mazurkiewicz, M., Niewiadomska, G., Wischik, C. M., Harrington, C. R., … Theuring, F. (2015). Different pathways of molecular pathophysiology underlie cognitive and motor tauopathy phenotypes in transgenic models for Alzheimer's disease and frontotemporal lobar degeneration. *Cellular and Molecular Life Sciences*, 72, 2199–2222. https://doi.org/10.1007/s00018-014-1804-z

Mena, R., Edwards, P., Pérez-Olvera, O., & Wischik, C. M. (1995). Monitoring pathological assembly of tau and beta-amyloid proteins in Alzheimer's disease. *Acta Neuropathologica*, 89, 50–56. https://doi.org/10.1007/BF00294259

Mesulam, M.-M. (2013). Cholinergic circuitry of the human nucleus basalis and its fate in Alzheimer's disease. *The Journal of Comparative Neurology*, 521, 4124–4144. https://doi.org/10.1002/cne.23415

Mesulam, M.-M., & van Hoesen, G. W. (1976). Acetylcholinesterase-rich projections from the basal forebrain of the rhesus monkey to neocortex. *Brain Research*, 109, 152–157. https://doi.org/10.1016/0006-8993(76)90385-1

Mohr, F., Krejci, E., Zimmermann, M., & Klein, J. (2015). Dysfunctional presynaptic M2 receptors in the presence of chronically high acetylcholine levels: Data from the PRiMA knockout mouse. *PLoS One*, https://doi.org/10.1371/journal.pone.0141136

Nair, A. B., & Jacob, S. (2016). A simple practical guide for dose conversion between animal and human. *Journal of Basic and Clinical Pharmacy*, 7, 27–31.

Ower, A. K., Hadjichrysanthou, C., Gras, L., Goudsmit, J., Anderson, R. M., & de Wolf, F. (2018). Temporal association patterns and dynamics of amyloid-β and tau in Alzheimer's disease. *European Journal of Epidemiology*, 33, 657–666. https://doi.org/10.1007/s10654-017-0326-z

Oz, M., Lorke, D. E., Hasan, M., & Petroianu, G. A. (2011). Cellular and molecular actions of Methylene Blue in the nervous system. *Medicinal Research Reviews*, 31, 93–117. https://doi.org/10.1002/med.20177

Pepeu, G., & Grazia Giovannini, M. (2017). The fate of the brain cholinergic neurons in neurodegenerative diseases. *Brain Research*, 1670, 173–184. https://doi.org/10.1016/j.brainres.2017.06.023

Pfaffendorf, M., Bruning, T. A., Batnik, H. D., & van Zwieten, P. A. (1997). The interaction between methylene blue and the cholinergic system. *British Journal of Pharmacology*, 122, 95–98. https://doi.org/10.1038/sj.bjp.0701355

Riedel, G., Klein, J., Niewiadomska, G., Kondak, C., Schwab, K., Lauer, D., Magbagbeolu, M., Steczkowska, M., Zadrozny, M., Wydrych, M., Cranston, A., Melis, V., Santos, R. X., Theuring, F., Harrington, C. R., & Wischik, C. M. (2020). Mechanisms of anticholinesterase interference with tau aggregation inhibitor activity in a tau-transgenic mouse model. *Current Alzheimer Research*, 17, 285–296. https://doi.org/10.2174/1567205017666200224120926

Sakanaka, M., Shiosaka, S., Takagi, H., Senba, E., Takatsuki, K., Inagaki, S., Yabuuchi, H., Matsuzaki, T., & Tohyama, M. (1980). Topographic organization of the projection from the forebrain subcortical areas to the hippocampal formation of the rat. *Neuroscience Letters*, 20, 253–257. https://doi.org/10.1016/0304-3940(80)90156-1

14714159, 2022, 2, Downloaded from https://onlinelibrary.wiley.com/doi/10.1111/jnc.15553 by Test, Wiley Online Library on [30/07/2024]. See the Terms and Conditions (https://onlinelibrary.wiley.com/terms-and-conditions) on Wiley Online Library for rules of use; OA articles are governed by the applicable Creative Commons License

Sarter, M., & Lustig, C. (2019). Cholinergic double duty: cue detection and attentional control. *Current Opinion in Psychology*, 29, 102–107. https://doi.org/10.1016/j.copsyc.2018.12.026

Schelter, B. O., Shiells, H., Baddeley, T. C., Rubino, C. M., Ganesan, H., Hammel, J., Vuksanovic, V., Staff, R. T., Murray, A. D., Bracoud, L., Riedel, G., Gauthier, S., Jia, J., Bentham, P., Kook, K., Storey, J. M. D., Harrington, C. R., & Wischik, C. M. (2019). Concentration-dependent activity of hydromethylthionine on cognitive decline and brain atrophy in mild to moderate Alzheimer's disease. *Journal of Alzheimer's Disease*, 72, 931–946. https://doi.org/10.3233/JAD-190772

Schirmer, R. H., Adler, H., Pickhardt, M., & Mandelkow, E. (2011). Lest we forget you—methylene blue…. *Neurobiology of Aging*, 32, 2325-e7. https://doi.org/10.1016/j.neurobiolaging.2010.12.012

Schliebs, R., & Arendt, T. (2006). The significance of the cholinergic system in the brain during aging and in Alzheimer's disease. *Journal of Neural Transmission*, 113, 1625–1644. https://doi.org/10.1007/s00702-006-0579-2

Schneider, L. S., Dagerman, K. S., Higgins, J. P. T., & McShane, R. (2011). Lack of evidence for the efficacy of memantine in mild Alzheimer disease. *Archives of Neurology*, 68, 991–998. https://doi.org/10.1001/archneurol.2011.69

Schwab, K., Frahm, S., Horsley, D., Rickard, J. E., Melis, V., Goatman, E. A., Magbagbeolu, M., Douglas, M., Leith, M. G., Baddeley, T. C., Storey, J. M. D., Riedel, G., Wischik, C. M., Harrington, C. R., & Theuring, F. (2017). A protein aggregation inhibitor, leuco-methylthioninium bis(hydromethanesulfonate), decreases α-synuclein inclusions in a transgenic mouse model of synucleinopathy. *Frontiers in Molecular Neuroscience*, 10, 447. https://doi.org/10.3389/fnmol.2017.00447

Spillantini, M. G., & Goedert, M. (2013). Tau pathology and neurodegeneration. *The Lancet Neurology*, 12, 609–622. https://doi.org/10.1016/S1474-4422(13)70090-5

Stein, C., Koch, K., Hopfeld, J., Lobentanzer, S., Lau, H., & Klein, J. (2019). Impaired hippocampal and thalamic acetylcholine release in P301L tau-transgenic mice. *Brain Research Bulletin*, 152, 134–142. https://doi.org/10.1016/j.brainresbull.2019.07.014

Thiele, A. (2013). Muscarinic signaling in the brain. *Annual Review of Neuroscience*, 36, 271–294. https://doi.org/10.1146/annurev-neuro-062012-170433

Tretter, L., Horvath, G., Hölgyesi, A., Essek, F., & Adam-Vizi, V. (2014). Enhanced hydrogen peroxide generation accompanies the beneficial bioenergetic effects of methylene blue in isolated brain mitochondria. *Free Radical Biology and Medicine*, 77, 317–330. https://doi.org/10.1016/j.freeradbiomed.2014.09.024

Vana, L., Kanaan, N. M., Ugwu, I. C., Wuu, J., Mufson, E. J., & Binder, L. I. (2011). Progression of tau pathology in cholinergic Basal forebrain neurons in mild cognitive impairment and Alzheimer's disease. *American Journal of Pathology*, 179, 2533–2550. https://doi.org/10.1016/j.ajpath.2011.07.044

Vertes, R. P., Albo, Z., & Di Viana, P. G. (2001). Theta-rhythmically firing neurons in the anterior thalamus: Implications for mnemonic functions of Papez's circuit. *Neuroscience*, 104, 619–625. https://doi.org/10.1016/s0306-4522(01)00131-2

Visarius, T. M., Stucki, J. W., & Lauterburg, B. H. (1997). Stimulation of respiration by methylene blue in rat liver mitochondria. *FEBS Letters*, 412, 157–160. https://doi.org/10.1016/S0014-5793(97)00767-9

Whitehouse, P. J., Price, D. L., Clark, A. W., Coyle, J. T., & DeLong, M. R. (1981). Alzheimer disease: Evidence for selective loss of cholinergic neurons in the nucleus basalis. *Annals of Neurology*, 10, 122–126. https://doi.org/10.1002/ana.410100203

Wilcock, G. K., Gauthier, S., Frisoni, G. B., Jia, J., Hardlund, J. H., Moebius, H. J., Bentham, P., Kook, K. A., Schelter, B. O., Wischik, D. J., Davis, C. S., Staff, R. T., Vuksanovic, V., Ahearn, T., Bracoud, L., Shamsi, K., Marek, K., Seibyl, J., Riedel, G., … Wischik, C. M. (2018). Potential of low dose leuco-methylthioninium bis(hydromethanesulphonate) (LMTM) monotherapy for treatment of mild Alzheimer's disease: Cohort analysis as modified primary outcome in a phase III clinical trial. *Journal of Alzheimer's Disease*, 61, 435–457. https://doi.org/10.3233/JAD-170560

Wischik, C. M., Edwards, P. C., Lai, R. Y., Gertz, H.-N.-J., Xuereb, J. H., Paykel, E. S., Brayne, C., Huppert, F. A., Mukaetova-Ladinska, E. B., Mena, R., Roth, M., & Harrington, C. R. (1995). Quantitative analysis of tau protein in paired helical filament preparations: Implications for the role of tau protein phosphorylation in PHF assembly in Alzheimer's disease. *Neurobiology of Aging*, 16, 409–417. https://doi.org/10.1016/0197-4580(95)97327-D

Wischik, C. M., Edwards, P. C., Lai, R. Y., Roth, M., & Harrington, C. R. (1996). Selective inhibition of Alzheimer disease-like tau aggregation by phenothiazines. *Proceedings of the National Academy of Sciences of the United States of America*, 93, 11213–11218. https://doi.org/10.1073/pnas.93.20.11213

Wischik, C. M., Novak, M., Thøgersen, H. C., Edwards, P. C., Runswick, M. J., Jakes, R., Walker, J. E., Milstein, C., Roth, M., & Klug, A. (1988). Isolation of a fragment of tau derived from the core of the paired helical filament of Alzheimer disease. *Proceedings of the National Academy of Sciences of the United States of America*, 85, 4506–4510. https://doi.org/10.1073/pnas.85.12.4506

Wischik, C. M., Staff, R. T., Wischik, D. J., Bentham, P., Murray, A. D., Storey, J. M. D., Kook, K. A., & Harrington, C. R. (2015). Tau aggregation inhibitor therapy: an exploratory phase 2 study in mild or moderate Alzheimer's disease. *Journal of Alzheimer's Disease*, 44, 705–720. https://doi.org/10.3233/JAD-142874

Zimmermann, M. (2020). *The diseased brain and the failing mind: Dementia in science, medicine and literature of the long twentieth century. Explorations in science and literature*. Bloomsbury Academic.

How to cite this article: Kondak, C., Riedel, G., Harrington, C. R., Wischik, C. M., & Klein, J. (2022). Hydromethylthionine enhancement of central cholinergic signalling is blocked by rivastigmine and memantine. *Journal of Neurochemistry*, 160, 172–184. https://doi.org/10.1111/jnc.15553

14714159, 2022, 2, Downloaded from https://onlinelibrary.wiley.com/doi/10.1111/jnc.15553 by Test, Wiley Online Library on [30/07/2024]. See the Terms and Conditions (https://onlinelibrary.wiley.com/terms-and-conditions) on Wiley Online Library for rules of use; OA articles are governed by the applicable Creative Commons License